



Roughness correlations in ultra-thin polymer blend films

J.S. Gutmann^a, P. Müller-Buschbaum^b, D.W. Schubert^c, N. Stribeck^d,
D. Smilgies^e, M. Stamm^{a,1,*}

^aMax-Planck-Institut für Polymerforschung, Ackermannweg 10, D-55128 Mainz, Germany

^bPhysik Department E13, TU-München, James-Frank-Straße 1, D-85747 Garching, Germany

^cGKSS Forschungszentrum, Max-Planck-Straße, D-20502 Geesthacht, Germany

^dInstitut TMC, Universität Hamburg, Bundesstraße 45, D-20146 Hamburg, Germany

^eESRF, BP 220, F-38043 Grenoble Cedex, France

Abstract

Ultra-thin films of weakly incompatible polymer blends form smooth films with correlated interfaces upon suitable preparation. With the poly-(styrene-co-para-bromo-styrene) $\text{PBr}_{0.91}\text{S}/\text{PBr}_{0.67}\text{S}$ blend system, of slightly different degrees of bromination, a series of samples with varying composition on top of roughened substrates has been investigated. The surface morphology of the thin films was characterized by microscopy measurements, while with diffuse X-ray scattering the roughness correlation between the interfaces was examined. A lower cut-off length of the replicated roughness spectrum at small dimensions was obtained. Our results show, that the blend composition has a distinct influence on the replicated in-plane lengths. © 2000 Elsevier Science B.V. All rights reserved.

PACS: 83.30.ES; 61.10.KW; 61.10.Eq; 68.55.-a

Keywords: Polymers; Ultra-thin films; Roughness correlations; Scattering

1. Introduction

Polymeric coatings find widespread use in many contemporary applications such as dielectric coatings and photoresists in the semiconductor industry or biocompatibilisation of surfaces. Since the individual functional requirements are very different it is a common practice to prepare the films from a mixture of two or more components in order to achieve the required properties. However, due to the low entropy of mixing, polymeric blends are mostly incompatible and phase separate under appropriate conditions. For ultra-thin films the additional

presence of a surface leads to a behaviour which is very different from bulk systems [1]. In incompatible polymer blends the thin film may undergo phase separation even during preparation. This behaviour has been observed in a variety of incompatible blend systems where phase separation perpendicular or parallel to the substrate was observed [2–10]. If the blended polymers are only weakly incompatible, the phase separation process may not be fast enough to allow a phase separation during the preparation process. In this case essentially smooth blend films are obtained over a wide compositional range.

While the case of interfacial correlation has previously been observed in single polymer films [11,12] and bilayer polymer films [13,14], we examine the interface correlation in ultra-thin binary-blend films of the statistical poly-(styrene-co-para-bromo-styrene) copolymers $\text{PBr}_{0.91}\text{S}$ (i.e. at 91% bromination) and $\text{PBr}_{0.67}\text{S}$. Using this very weakly incompatible blend system it is possible to prepare ultra-thin films with correlated interfaces by a suitable choice of preparation conditions such as the

* Corresponding author. Tel.: + 49-351-4658-0;-224;-225; fax: + 49-351-4658-284.

E-mail address: stamm@ipfdd.de, gutmann@mpip-mainz.mpg.de (J.S. Gutmann)

¹ Present address: Institut für Polymerforschung Dresden e.V., Hohe Straße 6, D-01069 Dresden, Germany.

used solvent and substrate, polymer concentration and composition as well as spinning speed. As shown in Fig. 1 the ultra-thin polymer-blend film forms a smooth layer which almost exactly replicates the topography of the substrate. However, only a part of the substrates roughness spectrum is replicated [15,12]. This replication process is essentially limited by the elastic properties of the polymer layer during the preparation process to the replication of in-plane length scales larger than a lower cut-off length. As a consequence of this, the interfaces of the ultra-thin polymer films are correlated on length scales larger than the lower cut-off length. The presence of this correlations alters the intensity distribution in reciprocal space. In the case of uncorrelated homogeneous films with a well-defined average thickness, the superposition of the scattering from the individual interfaces leads to intensity modulations (the so called Kiessig fringes) only along the q_z -axis of reciprocal space (with the q_x and q_y components of the scattering vector \mathbf{q} equal to 0). However in the case of interfacial correlations, the scattered intensity is spread out into sheets of enhanced intensity in reciprocal space whose extensions into the q_x and q_y direction are determined by the lower cut-off length of the replication process. This lower cut-off of the replicated roughness spectrum may be determined from the q_y dependence of the decay of the oscillations in the detector scan and off-detector scans (with q_y being the in-plane component of the scattering vector in y -direction, cf. Fig. 2). Thus, the diffuse X-ray scattering experiments yield an additional information that cannot be obtained by a microscopic investigation of the thin film (common microscopy techniques such as optical or scanning force microscopy lack the depth sensitivity of the scattering methods and are therefore intrinsically limited to investigations of the sample surface).

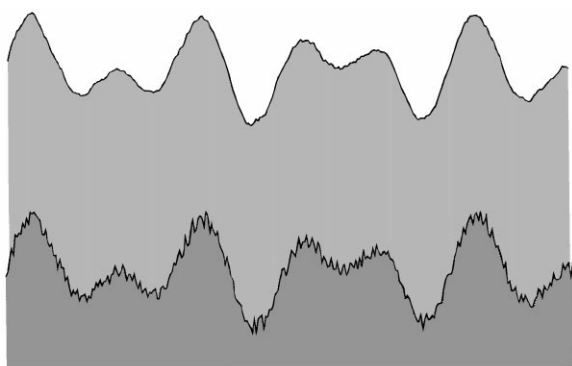


Fig. 1. Schematic drawing of a polymer film (light grey) with roughness correlations on top of a substrate (dark grey). The polymer film replicates the substrate features larger than a cutoff length. Thus only the low-frequency part of the substrates roughness spectrum is replicated.

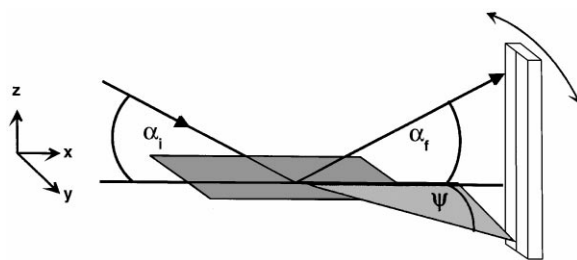


Fig. 2. Schematic drawing of the setup for scattering under grazing incidence at the ID10B beamline at ESRF. The incoming beam impinges on the sample under the grazing angle α_i . A 1D position-sensitive detector with crystal optics is used to record the scattered intensity. These vertical cuts (varying α_f) probe mainly q_z and are therefore well suited to determine interfacial correlations.

2. Experimental

2.1. Sample preparation

The statistical poly-(styrene-co-para-bromo-styrene) copolymers were prepared by a direct electrophilic bromination of protonated and deuterated polystyrene homopolymer precursors [16–19]. Both polystyrene precursors were prepared by anionic polymerization and were highly monodisperse, as determined by GPC. The brominated polystyrenes were characterized by DSC, the bromine content was calculated from microgravimetric analysis and the molecular weights were calculated on the basis of the polystyrene precursors molecular weight. The glass transition temperature of the polymers along with the other physical constants is summarized in Table 1.

As substrates we used silicon wafers (100 surface, manufacturer MEMC Electronic Materials Inc., Spartanburg). In order to enlarge the roughness spectrum of the substrates they were etched prior to spin coating in the following way. First, the wafers were stripped of the oxide layer, by dipping them into a 10% solution of hydrofluoric acid. Following a thorough rinse with Milli-Q water they were put into a 57% solution of potassium hydroxide (KOH) at 50°C which oxidizes the silicon and thus artificially roughens the surface. After 30 min the wafers were removed from the KOH solution, thoroughly rinsed with Milli-Q water and dried with compressed nitrogen.

The thin polymer-blend films were prepared by spin coating (2000 r.p.m., 30 s) a toluene solution of the polymer blend onto the roughend silicon substrates. All polymer-blend solutions were prepared with a total polymer concentration of 14.0 mg/ml and left to stir overnight to ensure complete dissolution. Within the $\text{PBr}_{0.91}\text{S}/\text{PBr}_{0.67}\text{S}$ -blend series the relative amount of both polymers was varied. The series comprises of five

Table 1

Characteristics of the polymers used in this study. Isotopic substitution is given for completeness only

Polymer	M_w (k)	M_w/M_n	T_g ($^{\circ}\text{C}$)
PBr _{0.91} S protonated	393	1.03	143.1
PBr _{0.67} S deuterated	364	1.04	135.3

samples with a PBr_{0.91}S mass fraction ϕ of 1.0, 0.9, 0.8, 0.7 and 0.6.

2.2. Microscopy measurements

The surface of the roughend substrates was characterized by optical microscopy using a Zygo Maxim 3D phase modulation interference microscope. The Maxim-3D uses optical interference from a laser beam in order to obtain a three-dimensional topography of the sample surface. By averaging over several measurements a depth resolution of about 7 Å is obtained. The sample itself was analyzed at different areas and from the individual topographies an average r.m.s.-roughness was calculated.

2.3. X-ray reflectivity measurements

The X-ray reflectivity measurements were conducted at a Seifert XTD 3003 TT X-ray diffraction system operated in reflectivity mode. A Ge(1 10) channel cut crystal was used as a monochromator at a fixed wavelength of $\lambda = 1.54$ Å. The reflectivity curves were analyzed by a fit to the data based on a Parratt formalism [20–22]. The layer interface were described by error function profiles, which are commonly used to describe the interfaces of polymer blends and substrates [23].

2.4. Diffuse X-ray scattering

Diffuse X-ray scattering measurements were carried out at the ID10B beamline of the ESRF storage ring in Grenoble. The setup for scattering in and out of the plane of reflection is shown in Fig. 2 and consisted of a custom made sample cell and a Si(1 1 1) monochromator in front of a one-dimensional linear detector which could be rotated around the z -axis (corresponding to the angle Ψ in Fig. 2). With a helium-filled sample-detector pathway of 671 mm and a wavelength of $\lambda = 1.548$ Å we were able to achieve an in-plane resolution of 4.96×10^{-4} Å⁻¹ (FWHM). The sample was placed onto a 2-axis goniometer with a z -translation table to allow the measurements in reflection geometry. This combination of high-flux, 1D detector and crystal optics allowed us to record the high-resolution scattering pictures at a fixed angle of incidence α_i . The scattering picture recorded in the detector scans ($\Psi = 0$) and off-detector scans ($\Psi \neq 0$)

comprises of both the specular reflected intensity and the off-specular scattered intensity with the Yoneda peak [24] and the oscillations due to conformal roughness as its most prominent features. As detailed in Ref. [15] the differential cross section for scattering from correlated interfaces is given by

$$\left(\frac{d\sigma}{d\Omega}\right)_{\text{diff}} = \frac{F\pi^2}{\lambda^4} \sum_{j,k=1}^m (n_j^2 - n_{j+1}^2)(n_k^2 - n_{k+1}^2)^* \times \sum_{h,l=0}^3 G_{h,j} G_{l,k}^* S_{j,k}^{h,l},$$

$$S_{j,k}^{h,l} = \exp\{-0.5[q_{h,j}^2 \sigma_j^2 + q_{l,k}^2 \sigma_k^2] - i[q_{h,j} z_j + q_{l,k}^* z_k]\} \times (q_{h,j} q_{l,k}^*)^{-1} \int_0^\infty dX \{\exp\{q_{h,j} q_{l,k}^* C_{j,k}(X)\} - 1\} \cos(q_x X),$$

where $C_{j,k}(X)$ is a displacement–displacement correlation function. Thus, in the case of a single correlated layer the summands (j,k) and their symmetric counterpart (k,j) interfere constructively with their scattered intensity, leading to sheets (or fringes in a one-dimensional cut) of enhanced intensity. These fringes are observable in the detector scan and are in-phase with the oscillations of the specular reflectivity. In the case of a single correlated layer the oscillations in the detector scan are therefore of the same width $\Delta q_z = 2\pi/d_{\text{layer}}$ as the Kiessig fringes in the specular scattered intensity of a layer of the thickness d_{layer} .

3. Results

The microscopic investigation of the roughened substrates revealed that the oxidation process resulted in a number of holes with various shapes and sizes. Since no preferential shape or size could be detected, the surface was only characterized in terms of its r.m.s.-roughness which was determined to be 25 Å. This roughening of the surface was also found in the reflectivity curves of the as prepared polymer blend-films, in which the Kiessig fringes were visibly damped. The analysis of the reflectivity curves via the Parratt formalism (cf. Fig. 3) however showed, that in order to achieve a reasonable agreement the r.m.s.-roughness of the substrate/blend-film interface and of the blend-film/air interface was noticeably smaller than the value obtained from the microscopy images (typically between 7 and 16 Å). This is due to the additional contributions of the scattering from the correlated interfaces which are not captured by the simple Parratt formalism. A complete fit of specular and diffuse scattering would be necessary to obtain the correct surface roughness values [25]. For this reason we restricted ourselves to the determination of the film thickness which was found to be of the order of 36 nm for all investigated polymer films (approximately two times the

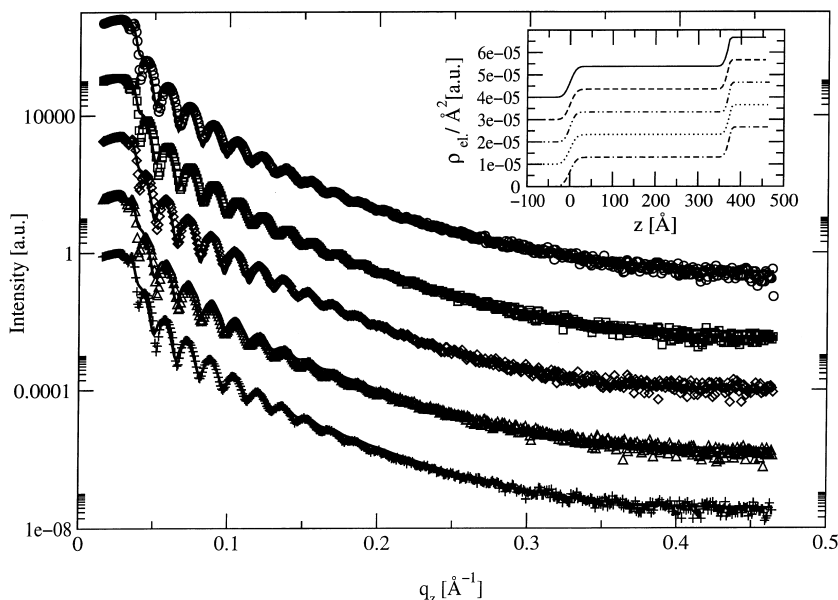


Fig. 3. Specular reflectivity curves of the investigated ultra-thin polymer films (symbols) and a fit based on a parratt formalism (solid lines). The corresponding scattering length profile is given in the inset. The blend composition decreases from the topmost ($\phi = 1$) to the bottom data-set ($\phi = 0.6$). Note that the curves are shifted with respect to each other for better visibility.

radius of gyration, R_g , of the blended polymers). Thus the investigated polymer films are truly ultra-thin. In the diffuse scattering experiments all polymer blend films showed clearly visible modulations in the detector scan and thus proved to exhibit conformal roughness. Fig. 4 shows a detector scan (topmost curve) along with off-detector scans (sorted with increasing q_y from top to bottom) for the sample with a composition of $\phi = 0.9$. Note that in order to decrease the noise levels in each individual scan, every single scan was smoothed by a running average of three data points. From the decay of the fringes the largest wave vector q_y^* at which fringes in the off-detectorscan, and correspondingly interfacial correlations, are present can be extracted. In real space the largest wave vector q_y^* corresponds to the lower cutoff length Λ which is given by $\Lambda = 2\pi/q_y^*$. Furthermore, it is immediately clear that in order to obtain the roughness correlations, the films were prepared in a regime of large values of dimensionless parameter Ω^2 which is given by the ratio of centrifugal to surface tensions forces [26,27].

Fig. 5 depicts the variation of Λ with the blend composition. Although the variations with the blend are small, it is clearly visible that the transition from a homo polymer-film ($\phi = 1$) to a blend film influences the lower cutoff length of the replicated roughness spectrum. While upon blending the smallest replicated length is initially shifted towards larger values it is afterwards steadily decreasing. This effect may either arises from a small change in the average elastic properties of the blended polymer film or from surface tension effects during spin

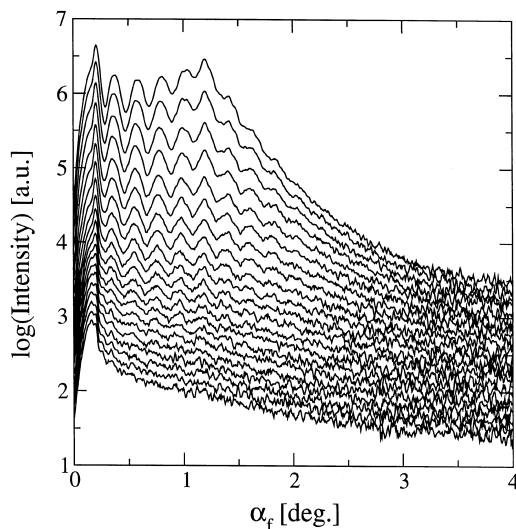


Fig. 4. Detector scans and off-detector scans for the polymer blend film containing 90 wt% $\text{PB}_{\text{r}0.91\text{S}}$ ($\phi = 0.9$). q_y increases from top ($q_y = 0 \text{ \AA}^{-1}$) to bottom ($q_y = 7.08 \times 10^{-3} \text{ \AA}^{-1}$) in steps of ($\Delta q_y = 3.54 \times 10^{-4} \text{ \AA}^{-1}$). The individual curves have been smoothed by a running average over three points, and are shifted with respect to each other for clarity.

coating. The elucidation of this question remains an open question, and will be addressed in future experiments. It is however clear that blending of polymers influences the replication of the roughness spectrum from the surface in a systematic way.

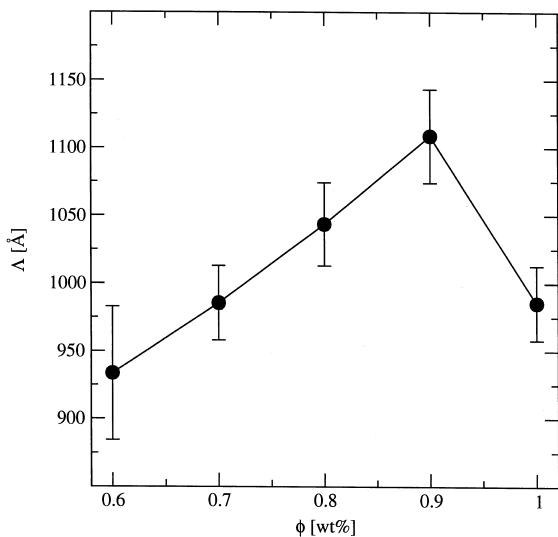


Fig. 5. Dependence of the smallest replicated in-plane length A on the blend composition ϕ in terms of wt% $\text{PBr}_{0.91}\text{S}$. The lines are given only as a guide to the eyes.

4. Conclusion

Ultra-thin polymer-blend films were prepared via spin coating of a mixture of the polymers in a common solvent onto artificially roughened substrates. With specular and diffuse X-ray scattering features of the thin films have been investigated, which are not accessible with the capabilities of ordinary microscopy methods, namely the partial replication of the roughness spectrum from the substrate surface to the surface of the ultra-thin polymer-blend film. From the presence of modulations which are in phase with the modulations in reflectivity measurements, we were able to conclude that a correlation of the interfaces is present. From the q_y dependence of the decay of the oscillations a lower cutoff length is determined which varies with blend composition.

Acknowledgements

We would like to thank J. Kraus and M. Wolkenhauer for their help during the diffuse X-ray experiments. J.S.G. would also like to acknowledge the financial support within the framework of the GKSS project V6.1.01.G.01-HS3.

References

- [1] G. Krausch, *Mater. Sci. Eng.* R14 (1995) 1.
- [2] S. Affrossman, G. Henn, S.A. O'Neill, R.A. Pethrick, M. Stamm, *Macromolecules* 29 (1996) 5010.
- [3] S. Affrossman, S.A. O'Neill, M. Stamm, *Macromolecules* 31 (1998) 6280.
- [4] D. Slep, J. Asselta, M.H. Rafailovich, J. Sokolov, D.A. Winsett, A.P. Smith, H. Ade, Y. Strzhemechny, S.A. Schwarz, B.B. Sauer, *Langmuir* 14 (1998) 4860.
- [5] A. Sung, A. Karim, J.F. Douglas, C.C. Han, *Phys. Rev. Lett.* 76 (1996) 4386.
- [6] K. Dalnoki-Veres, J.A. Forrest, J.R. Stevens, J.R. Dutcher, *Polym. Sci.* 34 (1996) 3017.
- [7] S. Walheim, M. Böltau, J. Mylnek, G. Krausch, U. Steiner, *Macromolecules* 30 (1997) 4996.
- [8] R.A.L. Jones, L.J. Norton, E.J. Kramer, F.S. Bates, P. Wiltzius, *Phys. Rev. Lett.* 66 (1991) 1326.
- [9] J.S. Gutmann, P. Müller-Buschbaum, M. Stamm, *Faraday Discuss.* 112 (1999) 285.
- [10] J.S. Gutmann, P. Müller-Buschbaum, D.W. Schubert, N. Stribeck, M. Stamm, *J. Macromol. Sci. Phys. Ed.* 38 (1999) 563.
- [11] P. Müller-Buschbaum, M. Stamm, *Macromolecules* 31 (1998) 3686.
- [12] P. Müller-Buschbaum, J.S. Gutmann, C. Lorenz, T. Schmidt, M. Stamm, *Macromolecules* 31 (1998) 9265.
- [13] J. Kraus, P. Müller-Buschbaum, D.G. Bucknall, M. Stamm, *J. Polym. Sci. Phys. Ed.* 37 (1999) 2862.
- [14] P. Müller-Buschbaum, J.S. Gutmann, J. Kraus, H. Walter, M. Stamm, *Macromolecules*, in press.
- [15] V. Holý, T. Baumbach, *Phys. Rev. B* 49 (1994) 10 668.
- [16] R.P. Kambour, J.T. Bandler, R.C. Bopp, *Macromolecules* 16 (1983) 753.
- [17] R.P. Kambour, J.T. Bandler, *Macromolecules* 19 (1986) 2679.
- [18] G.R. Strobl, J.T. Bandler, R.P. Kambour, A.R. Schultz, *Macromolecules* 19 (1986) 2683.
- [19] G. Krausch, M. Hipp, M. Boltau, O. Marti, J. Mlynek, *Macromolecules* 28 (1995) 260.
- [20] L.G. Parrat, *Phys. Rev.* 55 (1954) 359.
- [21] J. Leckner, *Theory of Reflection*, Martinus Nijhoff, Amsterdam, 1987.
- [22] M. Stamm, in: I.C. Sanches (Ed.), *Physics of Polymer Surfaces and Interfaces*, Butterworth-Heinemann, Boston, 1992.
- [23] M. Stamm, D.W. Schubert, *Annu. Rev. Mater. Sci.* 25 (1995) 325.
- [24] Y. Yoneda, *Phys. Rev.* 131 (1963) 2010.
- [25] J. Stettner, L. Schwalowsky, O.H. Seek, M. Tolan, W. Press, C. Schwarz, H.V. Känel, *Phys. Rev. B* 53 (1996) 1398.
- [26] F.-C. Chou, P.-Y. Wu, S.-C. Gong, *Jpn. J. Appl. Phys.* 37 (1998) 4321.
- [27] S.A. Gupta, R.K. Gupta, *Ind. Eng. Chem. Res.* 37 (1998) 2223.